Applied Surface Science 332 (2015) 756–760

Contents lists available at ScienceDirect

Applied Surface Science

journal homepage: www.elsevier.com/locate/apsusc

A new understanding of carbon nanotube growth: Different functions of carbon species

Yueling Zhang[a,*], Baojun Wang[b], Qing Yu[c], Yajun Tian[d]

[a] College of Engineering, Peking University, Summer Palace Road 5, Beijing 100871, PR China
[b] Key Laboratory of Coal Science and Technology, Taiyuan University of Technology, Yingze West Street 79, Taiyuan 030024, PR China
[c] School of Chemistry and Chemical Engineer and Center of Modern Analysis, Nanjing University, Hankou Road 22, Nanjing 210093, PR China
[d] National Institute of Clean-and-low-carbon Energy, P.O. Box 001 Shenhua NICE, Future Science & Technology Park, Beijing 102209, PR China

ARTICLE INFO

Article history:
Received 13 November 2014
Received in revised form 12 January 2015
Accepted 18 January 2015
Available online 24 January 2015

Keywords:
Chemical vapor deposition
Carbon nanotubes
Interface dynamics
Carbon species
Function

ABSTRACT

Understanding the formation mechanism of carbon nanotubes (CNTs) from carbon source is critical for controlled-production of CNTs. In this study, the functions of carbon species were investigated by a thermogravimetric analyzer coupled with a mass spectroscope in using methane as carbon source of CNT growth in chemical vapor deposition (CVD). It was found that a negative peak of C_2H_2 species and a positive peak of C_2H_4 species appeared at the CNT growth moment. Accordingly it is deduced that the C_2H_2 species react on nucleation and C_2H_4 species react on CNT growth. This deduction is then verified by the computational chemistry results based on density functional theory (DFT). This finding clarifies the different functions of C_2 at growing moment at the first time and makes the controlling of CNT production in such a condition becomes promising.

1. Introduction

Carbon nanotubes (CNTs) are important one-dimensional tubular carbon materials with unique structure and novel properties leading to potential applications in many fields [1–3]. CNTs can be synthesized by many approaches such as arc discharge [4] and laser ablation [5], among which chemical vapor decomposition (CVD) is a promising and versatile method with the advantages of moderate operational conditions and high-yield. However, the growth mechanism of CNTs in CVD system lagged behind very much. So far a lot of models have been proposed, but most of them explain CNT growth in macroscopic views [6–11] in which a carbon source is assumed to transform into 'carbon precursor', and then participates in the CNT growth, regardless of type of fed carbon source.

However, some research suggested the chemical structures of carbon play more important role in nanotube formation than their thermodynamic properties [12]. For example, the introduction of benzene species enhanced the growth of single-walled CNTs from methane [13], the pulse addition of C_2H_6 at the beginning of the CNT growth process effectively enhanced the single-walled CNT yield, indicating a special function of the C_2 species in CNT growth [14]. But it was unclear how the carbon species take part in the growth because the online evidence during CNT growth is difficult to obtain *in situ*. The mass production of CNTs by CVD requires scientific knowledge of the carbon species functions as guidance, so it is necessary to delve how the carbon species are involved, and what role the carbon species play in CNT growth.

Well-graphited and high productive quasi-aligned multi-walled CNTs have been produced by CVD method with benzene as carbon source in our previous work [15,16], and the activation and deactivation of catalyst were further revealed [17]. In this work a multi-walled CNT growth with methane as carbon source was performed in a thermogravimetric analyzer (TGA) coupled with a mass spectroscope (MS). With the analysis technique, the weight change and heat flow of the growth system were recorded by the TGA, meanwhile the changes of carbon species of the growth system could be recorded simultaneously online by the coupled mass spectrometer throughout the CNT growth time span. Based on the *in situ* results, the functions of C_2H_2 and C_2H_4 were identified, and it was further verified by thermodynamic principles.

2. Materials and methods

The catalysts with composition of $Ni_xMg_{1-x}MoO_4$ (Ni:Mg:Mo = 1:12:12) used in this study were prepared by the combustion method [16]. A thermogravimetric analyzer (STA-499C, NETZSCH), whose heating chamber serving as the reactor of CNT growth, is connected to a mass spectrometer (QUADSTAR-422, PFEIFFER) *via* a capillary tube with working temperature of 175 °C. The reactor was evacuated and purged

* Corresponding author. Tel.: +86 01062756633; fax: +86 01062756623.
E-mail address: zhangyueling1977@hotmail.com (Y. Zhang).

http://dx.doi.org/10.1016/j.apsusc.2015.01.117
0169-4332/

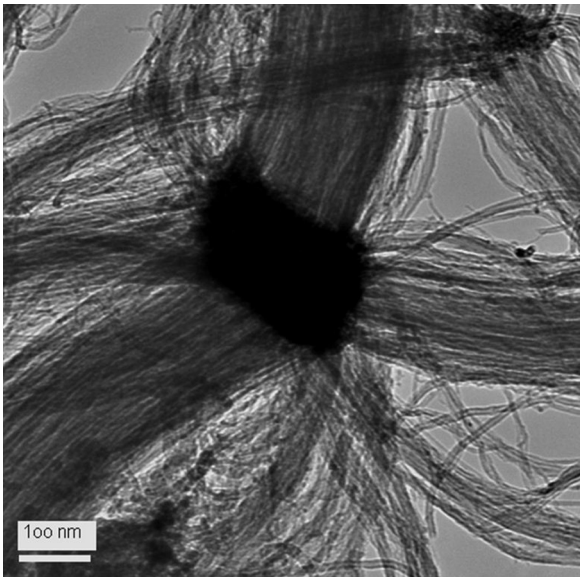

Fig. 1. TEM image of the CNT synthesized in thermogravimetric analyzer.

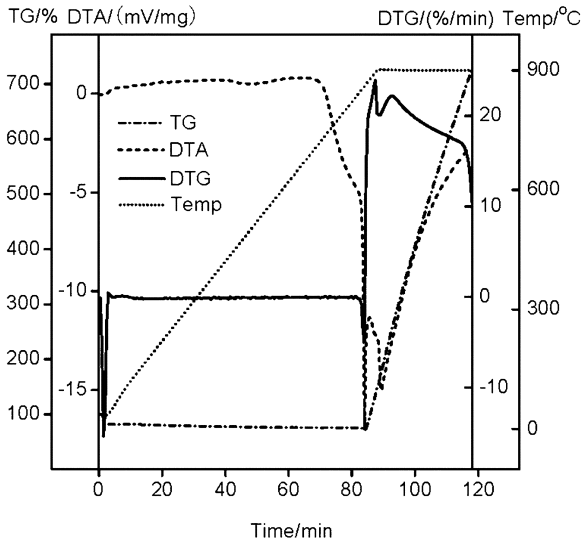

Fig. 2. TA profiles of the CNT growth of methane-CVD system with TG–MS technique.

several times before the experiment. Methane (99.999%, vol%) with a flow rate of 27 ml min^{-1} was loaded into the reactor where argon (99.999%, vol%) was used as a protection gas with a flow rate of 15 ml min^{-1}. The reactor was heated from room temperature to 900 °C at a heating rate of 10 °C min^{-1} at atmospheric pressure. The temperature was then fixed at 900 °C for 30 min. The simultaneous TGA and MS signals were recorded throughout the experiment running. A separate control experiment without catalyst was performed under the same conditions for comparison. Transmission electron microscope (TEM) was used for structural investigation of CNTs on a Tecnai-F20 field emission electron microscope with an accelerating voltage of 200 kV.

In the theoretical computation of the Gibbs energy of the CNT growth reactions, the $Dmol^3$ program [18] mounted on Materials Studio 4.0 package was used, and the Generalized Gradient Approximation (GGA) method with Becke One Parameter (BOP) function [19] was adopted at the Double Numerical plus d-functions (DND) basis level.

3. Results and discussion

3.1. TEM results

High-yield of CNTs were synthesized [15,16] in our experiments, Fig. 1 shows the TEM image of as-prepared product. It shows that well bundled and aligned CNTs develop radially from the surface of a catalyst particle. In the previous study, we have observed that the CNT developed with layered catalyst as substrate surface, and a macroscopic model well explaining high-yield production was proposed [15].

3.2. Thermal analysis results

Fig. 2 shows the TGA profiles of CNT growth. There is an obvious weight increase around 860 °C (84 min) in the thermogravimetric (TG) curve, indicating that the CNTs began to grow from this moment. Meanwhile, a rapid increase could be observed in the derivative thermogravimetry (DTG) curve, which denotes a sudden growth of CNTs. Moreover, the differential thermal analysis (DTA) was also performed, in which the curve appears a sharp endothermic peak before the growth caused by an alteration of catalyst ($Ni_xMg_{1-x}MoO_4$ to Ni–Mo/MgO) according to our previous analysis [16]. The growth proceeds for about 30 min, and a total yield as high as over 700% was achieved, while the activation and deactivation behaviors of growth are coincident with benzene-CVD system in inert atmosphere [17,20]. In summary, under such experimental conditions, the CNTs grow in a jump pattern at the time point of 84 min when the catalyst began to take effect.

3.3. Mass spectrum results

In order to investigate the gaseous carbon species resulted from CNT growth, we traced the ion currents of various hydrocarbon species by the mass spectrometer. The candidate species included alkane (16, 30, 44, 58, 72, 86 amu), olefin (28, 42, 56, 70, 84 amu), alkyne (26, 40, 50, 52, 54, 68, 82 amu) and arene (78, 92 amu). The ion current profiles of all traced species are presented in supporting information (see supplementary). Figs. 3 and 4 show the partial ion currents changes of H_2, C_2H_2 and C_2H_4, which obviously differ

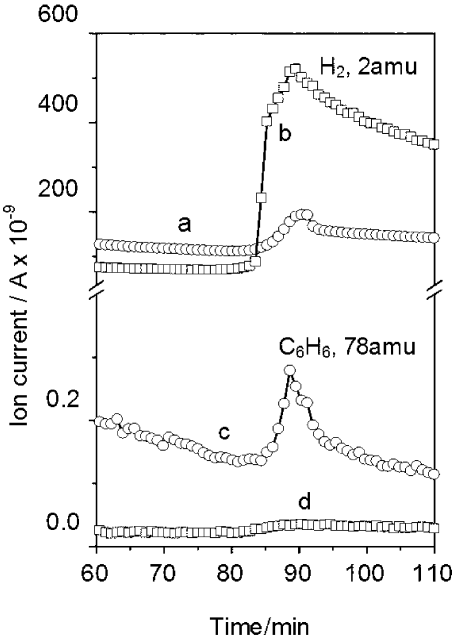

Fig. 3. Changes of ion current of H_2 and benzene during CNT growth. (□) Experimental data and (○) control data.

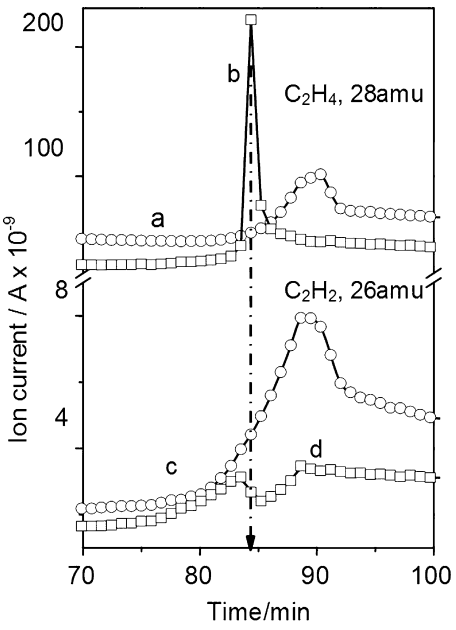

Fig. 4. Changes of ion currents of C_2H_4 and C_2H_2 during CNT growth. (□) Experimental data and (○) control data.

from other species in the absence and presence of catalyst. For comparison, the ion current changes of benzene (C_6H_6, 78 amu) were employed as a typical example to present a variation of other hydrocarbon species.

In the absence of catalyst (control experiment), H_2 was released at 86 min (Fig. 3a), corresponding to ~880 °C as displayed in Fig. 2. All the hydrocarbon species underwent similar variation trends in the control experiment. This phenomenon is consistent with a classic thermodynamic study on a simple methane pyrolysis process without catalyst in the system [21]. However, when the catalyst was present, not only the H_2 releasing temperature was lowered by about 20 °C (~860 °C, see Fig. 2 at 84 min) but the released amount of H_2 largely increased (Fig. 3b). The variation of H_2 species is attributed to the catalyst facilitating the activation of the C–H bond in CH_4, so that CNTs can grow at lower temperatures and a faster rate.

Most of other hydrocarbon species typically experienced a negligible variation as illustrated in Fig. 3d, except that C_2H_4 and C_2H_2 visibly varied at the CNT growth time (Fig. 4), C_2H_4 experienced a large-amplitude increasing process (Fig. 4b), while the C_2H_2 underwent a decreasing process (Fig. 4d). As indicated by the arrow in Fig. 4, C_2H_2 began to reduce but C_2H_4 began to accumulate prior to the growth point (~84 min). After this point, C_2H_4 species decreased and C_2H_2 increased, yet both them reached their respective equilibrium finally. This implies that C_2H_2 and C_2H_4 play different parts around the CNT growing point.

3.4. Discussion

It is known that the electron cloud of C_2H_2 is cylindrical and centrally symmetric with a σ C–C bond, while the electron cloud of C_2H_4 is axisymmetrically distributed above and below the σ C–C bond. Molecular attraction resulted from electro spin is liable to make the C–C bonds of C_2H_2 attract in the way of 'end to end' and form a polyyne ring [22]. According to the negative peak of C_2H_2 at growing point (Fig. 4d), it suggested that the polyyne ring constructed by C_2H_2 to be a precursor of the crystalnucleus of CNT growth. While the unit molecular structure (C–C bond length, hybrid orbital) of C_2H_4 (1.33 Å, sp^2) approximates to that of CNT (1.42 Å, sp^2), the sp^2 C_2 species has been found as a key precursor for the efficient growth of single-wall CNTs by CVD [23], which makes C_2H_4 easily congregate and form the structure of CNT, so the C_2H_4 peak disappeared rapidly in this stage (Fig. 4b). It is easy to understand that the catalyst could not be activated at one moment, so the two C_2 species react almost at the same time as illustrated in Fig. 4.

Based on the experimental results and corresponding analysis, a growth route of CNTs was proposed and a schematic figure of a ring with 12 carbon atoms is shown in Fig. 5. When the reactor is heated to high temperature many carbon species including C_2H_2 and C_2H_4 are generated by thermodynamics. As the catalyst is activated around 860 °C the C_2H_2 species aggregate in the way of 'end to end' (Fig. 5a), then polyyne rings are formatted over the catalyst (Fig. 5b), a polyyne ring is transformed into a steric carbon-ring of the polyyne (optimized by Gaussian 98 with B3LYP method at 6-31G* basis level), and a nucleus was formatted (Fig. 5c). Once the crystal nucleation is accomplished, C_2H_4 is then preferentially incorporated into carbon network for successive structural evolution of CNT (Fig. 5d–f). The formation of concentric polyyne rings with different diameters may evolve into multi-walled CNTs.

4. Thermodynamic analysis

In order to examine the credibility of the model, the reaction Gibbs energies of C_2H_4 and C_2H_2 as the precursor of CNT growth were further estimated by density functional theory (DFT), respectively. Referring to Fig. 5, for the Gibbs energy of step (a)→ step (c) at 860 °C (1133 K): the standard reaction entropy ($\Delta_r S^\circ$) and standard reaction enthalpy ($\Delta_r H^\circ$) at starting temperature can be calculated, and then the reaction Gibbs energy ($\Delta_r G^\circ$) at 1133 K can be calculated according to Eq. (1).

$$\Delta_r G^0_{1133\,K} = \Delta_r H^0_{1133\,K} + 1133 \cdot \Delta_r S^0_{1133\,K} \quad (1)$$

The $\Delta_r G^\circ$ with C_2H_2 and C_2H_4 as the precursor are $-105.57\ kJ\ mol^{-1}$ and $255.61\ kJ\ mol^{-1}$, respectively.

For the Gibbs energy of step (a)→ step (c) at 1133 K: the Gibbs energy of the reaction was calculated according to Eq. (2).

$$\Delta_r G_{1133\,K} = \Delta_r G^0_{1133\,K} + RT\ \ln\ Q_P \quad (2)$$

When the growth of CNTs starts, raw material is reacted and new species is generated, so the partial pressure of the gaseous substances must be taken into account. With C_2H_4 as the precursor, the reaction of step (c)→ step (d) is as 'C_2H_4 + nucleus = nucleus – C_2 + $2H_2$', and then Q_p can be calculated by Eq. (3).

$$Q_P = \frac{(p_{H_2}/p^0)^2}{(p_{C_2H_4}/p^0)} \quad (3)$$

where, p^0 is the atmospheric pressure. With C_2H_2 as the precursor, the reaction of step (c)→ step (d) is as 'C_2H_2 + nucleus = nucleus-C_2 + H_2', and then Q_p can be calculated by Eq. (4).

$$Q_P = \frac{(p_{H_2}/p^0)}{(p_{C_2H_2}/p^0)} \quad (4)$$

The difference of Gibbs energy of two reactions is obtained by Eq. (5).

$$\Delta_r G_{1133\,K,C_2H_4} - \Delta_r G_{1133\,K,C_2H_2} = (\Delta_r G^0_{1133\,K,C_2H_4} - \Delta_r G^0_{1133\,K,C_2H_2}) + RT\ \ln\left(\frac{(p_{C_2H_2}/p^0)(p_{H_2}/p^0)}{p_{C_2H_4}/p^0}\right) \quad (5)$$

According to the gas chromatography measurement (Agilent 9610), the maximum H_2 volume concentration is less than 10% (5.6, vol%), and the mass spectra signal intensity (Fig. 4) indicates

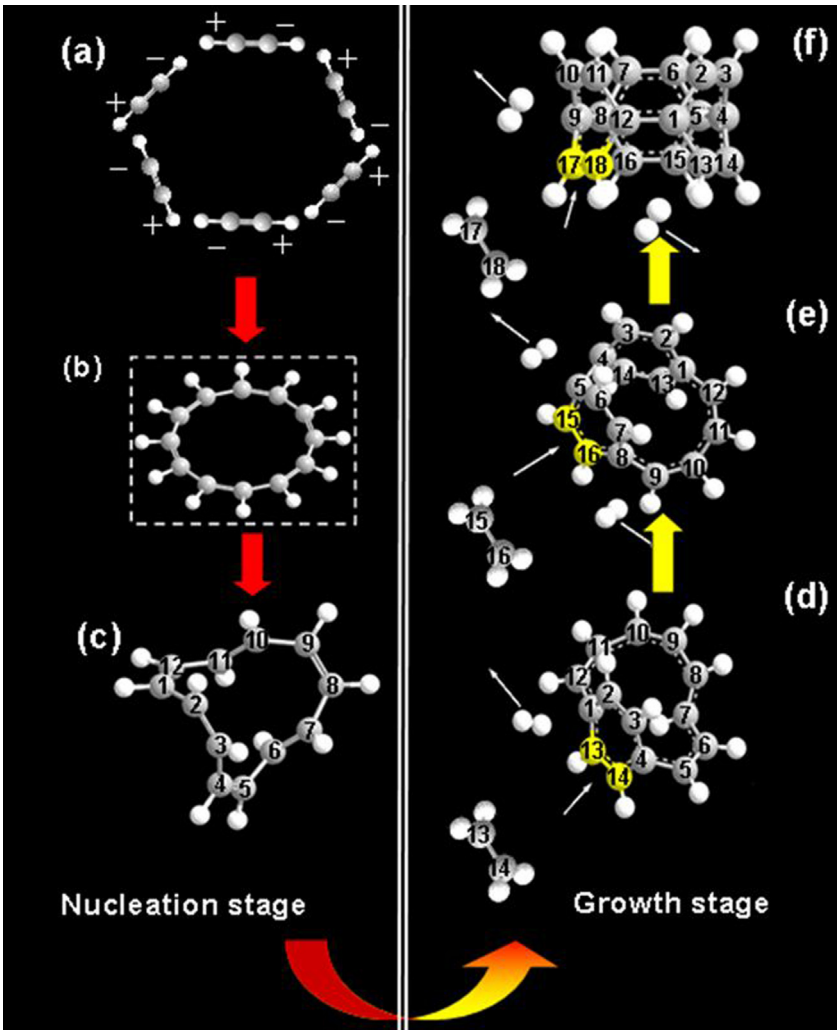

Fig. 5. Schematic diagram of a C_2-species involved CNT growth. Gray dots denote C atoms and white dots denote H atoms.

the mol ratio of C_2H_2 to C_2H_4 at the growth point is less than 0.01, namely, $p_{H_2}/p^0 < 0.1$, and $(p_{C_2H_2}/p^0)/(p_{C_2H_4}/p^0) < 0.01$. So, $\Delta_r G_{1133\,K,C_2H_4} - \Delta_r G_{1133\,K,C_2H_2} < 4.88\,kJ\ mol^{-1}$. It concludes that $\Delta_r G_{1133\,K,C_2H_4} < \Delta_r G_{1133\,K,C_2H_2}$.

In the nucleation step (a)→(c), no growth of CNT takes place; the reaction pathway is determined by their standard reaction Gibbs energies. Because the $\Delta_r G^\circ$ with C_2H_2 as precursor is far less than that with C_2H_4, C_2H_2 species is the prior precursor for nucleation reaction. In the growth step of (c)→(d), it is evident that the reaction Gibbs energies with C_2H_4 as precursor are smaller than that with C_2H_2, showing that C_2H_4 is the preferred candidate in this step, same conclusions are derived for the steps of (d)→(e) and (e)→(f). It is suggested that C_2H_4 species are preferred in the following CNT growth stage. While the thermodynamic analysis strongly supports the proposed C_2 species play different roles in the growing point of CNTs, C_2H_2 species reacts on nucleation and C_2H_4 species reacts on CNT development. This is the major reason that CNT growth is efficiently improved when C_2 species were introduced in many works [12,23–25].

5. Conclusions

In summary, both the experimental evidence and the thermodynamic analysis support the new understanding that there exist function divisions of carbon species in the CNT growing moment. Specifically, C_2H_2 species contribute the CNT nucleation and C_2H_4 species contribute the follow-up growth after nucleation. This study of CNT growth not only provides a new insight for CNT formation, but also offers a reliable detection method *in situ* for the further investigations of other carbon sources.

Acknowledgment

The work reported here is financially supported by the National Natural Science Foundation of China (Nos. 20506010).

Appendix A. Supplementary data

Supplementary data associated with this article can be found, in the online version, at http://dx.doi.org/10.1016/j.apsusc.2015.01.117.

References

[1] R.H. Baughman, A.A. Zakhidov, W.A. de Heer, Carbon nanotubes – the route toward applications, Science 297 (2002) 787–792.
[2] J.H. Hafner, C.L. Cheung, C.M. Lieber, Growth of nanotubes for probe microscopy tips, Nature 398 (1999) 761–762.
[3] J. Kong, N.R. Franklin, C. Zhou, M.G. Chapline, S. Peng, K. Cho, H. Dai, Nanotube molecular wires as chemical sensors, Science 287 (2000) 622–625.

[4] T.W. Ebbesen, P.M. Ajayan, Large-scale synthesis of carbon nanotubes, Nature 358 (1992) 220–222.
[5] T. Guo, P. Nikolaev, A.G. Rinzler, D. Tomanek, D.T. Colbert, R.E. Smalley, Self-assembly of tubular fullerenes, J. Phys. Chem. 99 (1995) 10694–10697.
[6] R. Saito, M. Fujita, G. Dresselhaus, M.S. Dresselhaus, Electronic structure and growth mechanism of carbon tubules, Mater. Sci. Eng. B: Solid-State Mater. Adv. Technol. 19 (1993) 185–191.
[7] M. Endo, H.W. Kroto, Formation of carbon nanofibers, J. Phys. Chem. 96 (1992) 6941–6944.
[8] T. Hayashi, Y.A. Kim, T. Matoba, M. Esaka, K. Nishimura, T. Tsukada, M. Endo, M.S. Dresselhaus, Smallest freestanding single-walled carbon nanotube, Nano Lett. 3 (2003) 887–889.
[9] R.S. Wagner, W.C. Ellis, Vapor–liquid–solid mechanism of single crystal growth, Appl. Phys. Lett. 4 (1964) 89–90.
[10] A. Gorbunov, O. Jost, W. Pompe, A. Graff, Solid–liquid–solid growth mechanism of single-wall carbon nanotubes, Carbon 40 (2002) 113–118.
[11] G.X. Du, S.A. Feng, J.H. Zhao, C. Song, S.L. Bai, Z.P. Zhu, Particle-wire-tube mechanism for carbon nanotube evolution, J. Am. Chem. Soc. 128 (2006) 15405–15414.
[12] Q.W. Li, H. Yan, J. Zhang, Z.F. Liu, Effect of hydrocarbons precursors on the formation of carbon nanotubes in chemical vapor deposition, Carbon 42 (2004) 829–835.
[13] N.R. Franklin, H.J. Dai, An enhanced CVD approach to extensive nanotube networks with directionality, Adv. Mater. 12 (2000) 890–894.
[14] H. Qi, D.N. Yuan, J. Liu, Two-stage growth of single-walled carbon nanotubes, J. Phys. Chem. C 111 (2007) 6158–6160.
[15] Y.J. Tian, H.X. Yang, Y.B. Cui, S.L. Zhan, Y.F. Chen, A multi-stage growth model leading to high-yield production of carbon nanotubes, Chem. Commun. (2008) 3299–3301.
[16] S. Zhan, Y. Tian, Y. Cui, H. Wu, Y. Wang, S. Ye, Y. Chen, Effect of process conditions on the synthesis of carbon nanotubes by catalytic decomposition of methane, China Particuol. 5 (2007) 213–219.
[17] Y. Zhang, Q. Yu, X. Wang, Y. Tian, A new understanding of carbon nanotube growth: activation and deactivation of a catalyst, Appl. Surf. Sci. 298 (2014) 221–224.
[18] B. Delley, From molecules to solids with the Dmol3 approach, J. Chem. Phys. 113 (2000).
[19] T. Tsuneda, T. Suzumura, K. Hirao, A new one-parameter progressive Colle–Salvetti-type correlation functional, J. Chem. Phys. 110 (1999) 10664–10678.
[20] Y. Tian, Z. Hu, Y. Yang, X. Wang, X. Chen, H. Xu, Q. Wu, W. Ji, Y. Chen, In situ TA–MS study of the six-membered-ring-based growth of carbon nanotubes with benzene precursor, J. Am. Chem. Soc. 126 (2004) 1180–1183.
[21] J.E. Germain, C. Vaniscotte, Craquage du methane dans un reacteur tubulaire. 1. Effet du rapport surface-volume, Bull. Soc. Chim. Fr. (1957) 692–695.
[22] C.H. Kiang, W.A. Goddard, Polyyne ring nucleus growth model for single-layer carbon nanotubes, Phys. Rev. Lett. 76 (1996) 2515–2518.
[23] B. Shukla, T. Saito, M. Yumura, S. Iijima, An efficient carbon precursor for gas phase growth of SWCNTs, Chem. Commun. (2009) 3422–3424.
[24] W.Z. Qian, T. Tian, C.Y. Guo, Q. Wen, K.J. Li, H.B. Zhang, H.B. Shi, D.Z. Wang, Y. Liu, Q. Zhang, Y.X. Zhang, F. Wei, Z.W. Wang, X.D. Li, Y.D. Li, Enhanced activation and decomposition of CH_4 by the addition of C_2H_4 or C_2H_2 for hydrogen and carbon nanotube production, J. Phys. Chem. C 112 (2008) 7588–7593.
[25] R. Xiang, E. Einarsson, J. Okawa, Y. Miyauchi, S. Maruyama, Acetylene-accelerated alcohol catalytic chemical vapor deposition growth of vertically aligned single-walled carbon nanotubes, J. Phys. Chem. C 113 (2009) 7511–7515.